MICROCOPY RESOLUTION TEST CHART
NATIONAL BUREAU OF STANDARDS-1963-A

ADA130527

REPORT DOCUMENTATION PAGE		READ INSTRUCTIONS BEFORE COMPLETING FORM
1 REPORT NUMBER TR-83-02	2 GOVT ACCESSION NO. AD A130527	3 RECIPIENT'S CATALOG NUMBER
4 TITLE (and Subtitle) Vibrational Spectra of Single and Mixed Alkali Pentasilicate Glasses		5 TYPE OF REPORT & PERIOD COVERED Technical
		6 PERFORMING ORG. REPORT NUMBER
7 AUTHOR(s) Efstratios I. Kamitsos and William M. Risen, Jr.		8 CONTRACT OR GRANT NUMBER(s) N00014-75-C-0883 NR-051-539
9 PERFORMING ORGANIZATION NAME AND ADDRESS Department of Chemistry Brown University Providence, Rhode Island 02912		10 PROGRAM ELEMENT, PROJECT, TASK AREA & WORK UNIT NUMBERS ONR-N00014-75-C-0883 NR-051-539
11 CONTROLLING OFFICE NAME AND ADDRESS Office of Naval Research United States Navy		12 REPORT DATE May 20, 1983
		13 NUMBER OF PAGES 40
14 MONITORING AGENCY NAME & ADDRESS(If different from Controlling Office)		15 SECURITY CLASS (of this report)
		15a. DECLASSIFICATION/DOWNGRADING SCHEDULE

16 DISTRIBUTION STATEMENT (of this Report)

Distribution Unlimited; Approved for Public Release

17 DISTRIBUTION STATEMENT (of the abstract entered in Block 20, if different from Report)

18 SUPPLEMENTARY NOTES

19 KEY WORDS (Continue on reverse side if necessary and identify by block number)
Glasses, ionic conduction, mechanical properties, Raman, infrared, far infrared, silicate, mixed alkali, annealing, glass formation

20 ABSTRACT (Continue on reverse side if necessary and identify by block number)
The far infrared and laser Raman spectra of single and mixed alkali pentasilicate glasses, $M_2O \cdot 5SiO_2$ (M = Na, K, Rb, Cs) and $xCs_2O(1-x)Na_2O \cdot 5SiO_2$, are reported in both the annealed and unannealed forms. Study of the cation-motion bands in the far infrared shows that the vibrationally significant cation-network interactions are unaffected by either introduction of a second cation or by annealing, and these results are discussed in terms of the glass formation and annealing. The spectra of the network show the existence of intrinsic network strain, changes in distributions of bond angles related to alkali

DD FORM 1473 EDITION OF 1 NOV 68 IS OBSOLETE
S/N 0102-014-6601

DTIC FILE COPY

20. Continued

mixing and annealing, and evidence for the nature of the distribution of cations in the glass. The results are discussed in relation to the composition dependence of other properties of these and related mixed alkali glasses.

Vibrational Spectra of Single and Mixed Alkali Pentasilicate Glasses

Efstratios I. Kamitsos and William M. Risen, Jr.

Department of Chemistry

Brown University

Providence, Rhode Island 02912

Abstract

The far infrared and laser Raman spectra of single and mixed alkali pentasilicate glasses, $M_2O \cdot 5SiO_2$ (M = Na, K, Rb, Cs), and $xCs_2O(1-x)Na_2O \cdot 5SiO_2$ are reported in both the annealed and unannealed forms. Study of the cation-motion bands in the far infrared shows that the vibrationally significant cation-network interactions are unaffected by either introduction of a second cation or by annealing, and these results are discussed in terms of the glass formation and annealing. The spectra of the network show the existence of intrinsic network strain, changes in distributions of bond angles related to alkali mixing and annealing, and evidence for the nature of the distribution of cations in the glass. The results are discussed in relation to the composition dependence of other properties of these and related mixed alkali glasses.

Introduction

Mixed alkali glasses, which have the general formula $xM_2O(1-x)M_2'O \cdot yA_pO_q$ (where M_2O and $M_2'O$ are alkali metal oxides, and A_pO_q is a network former), are of special interest because many of their properties (1,2) vary extremely nonlinearly with x. This nonlinear behavior, viewed as resulting from the addition of the second alkali to an alkali oxide-containing glass, is known as the mixed alkali effect (MAE).

A number of authors (3-8) have proposed theories or models to explain certain mixed alkali effects, usually effects on a particular type of property such as electrical conductivity or internal friction. The MAE is quite pronounced in these cases, but it can be observed on a range of properties. This suggests that the different manifestations of the MAE may have a common origin, so it is important for a successful theory to address the effect on such a range of properties. This is a demanding requirement, and it is not surprising that no explanation has yet been applied to all manifestations of the MAE since many of the most pertinent MAE observations have been made on systems for which complementary information from other techniques is not available.

Not much systematic experimental data is available on either the structure of mixed alkali glasses (MAGs), which can be probed effectively by Raman spectroscopy, or the atomic scale interactions that are relevant to mixed alkali phenomena, such as those involving cation-cation and cation-network interactions and their variations with composition. Far infrared spectroscopy is useful for probing the interactions of cations with their local environments in glasses and other disordered condensed phases (9-12), but only one systematic investigation of such spectra of a series of MAGs has been reported (12).

We report here the results of a study of the far infrared and Raman spectra of a series of MAGs represented by $xCs_2O(1-x)Na_2O \cdot 5SiO_2$. To assist in identifying and assigning spectral features due to the presence of the two dissimilar

cations, the spectra of the corresponding single alkali glasses (SAGs),
$M_2O \cdot 5SiO_2$ (M = Li, Na, K, Rb, Cs) also have been studied. Influences of the
simultaneous presence of both cations on the structure of the glass should be
apparent in the spectra of the MAGs but absent in those of the SAGs.

One reason for choosing this particular Cs-Na pentasilicate mixed alkali
glass series for vibrational study is that our study of it by Brillouin
spectroscopy (13) showed that although the sound velocities and related elastic
constants vary nearly linearly with x, significant non-linearities are exhibited
by the Landau-Placzek ratio and the isothermal compressibility. The latter,
$K_{T,0}(T_f)$, the static isothermal compressibility at the fictive temperature,
exhibits a well defined minimum as a function of x, at x ≈ 0.5. The vibrational
Raman spectra of these glasses would be particularly helpful in understanding
the origin of the MAE if they can show whether or not this variation of
$K_{T,0}(T_f)$ with x is a reflection of a variation of structural features. While
Raman spectroscopy is useful for exploring network structures, the interactions
between cations and the network give rise to bands in the far infrared spectrum
(11,14), so far infrared spectroscopy has been used to probe any composition
dependence of cation motion. The other principal reason for studying this
Cs-Na MAG series is that others of its properties, such as electrical conducti-
vity and thermal conductivity as well as thermal diffusivity (15-17), have
been reported, and its composition is close to that of other silicate MAGs whose
mechanical properties have been investigated (18-20a).

Mixed alkali glasses have been reported to exhibit unique mechanical relaxa-
tional phenomena. Their mechanical spectra, in the form of the variation of
internal friction (tan δ) versus temperature, are quite different from those of
SAGs. It is useful to consider this mechanical MAE, the variation of the spectra

with x, to see how the vibrational spectra could be helpful in understanding these properties. Two main effects are observed in the mechanical MAE. First, the lowest temperature peak (LTP) in each spectrum, often called the "single alkali" peak, decreases in intensity and shifts to higher temperature as x increases from 0 to 0.5. Second, the high temperature peak (HTP), often called the "mixed alkali" peak, increases in intensity and shifts to lower temperature as this variation is made. There is some agreement that the LTP and the electrical losses, associated with the decrease in dc conductivity as x is varied, are due to the same type of mechanism, although the exact nature of it has not been agreed upon. In the case of the HTP, a number of different explanations have been suggested. According to one it depends on the mobility of the less mobile ion (18), and according to others it is explained in terms of the cooperative movement of both types of cations, which somehow interact (20).

In a recent analysis (21) of the data on the mechanical properties of MAGs, especially trisilicates, $xM_2O(1-x)M_2'O \cdot 3SiO_2$, it was found that the activation energies of the LTP are nearly the same as those for ionic conductivity and have maxima with respect to x in the 0.2 to 0.5 region. Simultaneously, the magnitude of tan δ exhibits a minimum with respect to x. The explanation given for the LTP is that it is due primarily to cooperative motion of cations, which involves ionic migration under the influence of a mechanical field that is similar to ionic migration in an electrical field. In this process, the network segments undergo only small amplitude displacements. The study of the far infrared spectra of these alkali pentasilicate MAGs and SAGs should provide information about the cation-anionic site interactions and the degree to which they depend on alkali composition.

In contrast, the HTP activation energy in MAGs shows a minimum as x is varied, but it is larger than the LTP activation energy at all MAG compositions. The magnitude of tan δ shows a maximum, though not at exactly the same composition.

In the analysis (21) it was suggested that the HTP is due to rearrangements of larger units, which involve both backbone segments and the neighboring cations and which exist in MAGs because of the strain resulting from the need of neighboring anionic sites to accommodate the size mismatch of the dissimilar cations. The strain induced into the system must be maximized at $x = 0.5$, since the probability of having two dissimilar cations next to each other is maximized at this composition. The minimum in the isothermal compressibility, expressed as $K_{T,0}(T_f)$, of $xCs_2O(1-x)Na_2O \cdot 5SiO_2$ also occurs at $x \approx 0.5$ (13). This probably indicates that the network of the glass with composition $x \approx 0.5$ has a minimum ability for local structural rearrangements and thus it is the most strained.

Strains giving rise to changes in bond angles and lengths or to changes in the distributions of these angles and lengths should be reflected in changes in the position or shapes of the Raman bands. The type of strain postulated as being due to cation-size mismatch should be present in both annealed and unannealed glasses, but other sources of strain in unannealed glasses could lead to analogous spectral features due to distributions in bond lengths and angles. The degree of strain related to the latter sources can be reduced significantly by annealing (22), but strain inherent to the structure of network segments resulting from cation-size differences would not be relieved by annealing unless cation segregation occurs. This forms the basis for studying the nature of the strains and the effects of annealing in these glasses by Raman spectroscopy.

The combined results of recently reported studies by differential scanning calorimetry, positron annihilation, and X-ray fluorescence methods further indicate that Raman and far infrared studies should be useful. They have been interpreted to mean that Si-O bond lengths are less in MAGs than in SAGs, while the Si-O bond energy and "covalence degree" are greater (23). It also was found that the M...O distance in MAGs is less, on average, than in the

corresponding SAGs. If these results demonstrate common phenomena in MAGs, they should be manifested in the spectra of the pentasilicate systems under investigation as well. The differences in Si-O bond length and energy should affect the Raman spectra while differences in M...O distances should affect the far infrared results.

Experimental Section

The Raman Spectra of three types of alkali pentasilicate samples, which are designated conveniently by their shapes as cube-shaped samples (cubes), fibers and chips, have been measured.

The preparation of the cubes of composition $xCs_2O(1-x)Na_2O \cdot 5SiO_2$ has been reported (13). The samples studied were the same as those on which the Brillouin measurements were performed. The main characteristic of the cube-shaped samples is that they were prepared such that after removal from the furnace the melts were allowed to cool to room temperature slowly and, after this step, the samples still in the crucibles were annealed at temperatures about 10°C above T_g. The glass transition temperatures of glasses in this series are given in reference 13.

The fibers and chips were prepared from the stoichiometrical appropriate amounts of reagent grade SiO_2, in the form of silicic acid, $SiO_2(H_2O)_x$, Na_2CO_3 and Cs_2CO_3. After the finely powdered components were mixed mechanically, the mixture was melted in a Pt crucible at 1550°C, in an open air electric furnace. The melts were stirred several times with a platinum wire and left in the furnace for about 30 h. This procedure produced clear, homogeneous melts from each composition, except of $Li_2O \cdot 5SiO_2$ which gave a phase-separated material. After their removal from the furnace, fibers 0.5 - 1.0 mm in diameter were drawn from the melts with the Pt wire. Immediately after the fibers were drawn, each crucible, containing the rest of the melt, was partially dipped into cold water

to quench the melts and obtain odd-shaped pieces (chips) of glass. The drawn
fibers and chips were used as specimens for Raman measurements without further
treatment. After Raman measurements were made on these chips, they were
annealed, and the Raman spectra of the annealed glasses were obtained.

Raman spectra were measured on a Jarrell-Ash 25-300 spectrometer. The source
was the 514.5 nm line of a Spectra Physics 165 Argon-ion laser operating at
about 1W. A 90° scattering geometry was employed and, in the case of fibers,
they were oriented such that their cross section was perpendicular to the
excitation beam. The spectral accuracy was ca 2 cm^{-1}. For the measurements of
depolarization ratios a Polaroid sheet was used as analyzer, and a scrambler
was placed in front of the entrance slit of the spectrometer to compensate for
the differences in the response of the gratings for different polarizations
of the entering light. The plane of polarization of the incident light was
controlled by a Spectra-Physics 310-21 Polarization Rotator.

The samples for the far IR measurements were prepared by grinding chips in
a Wig-L-Bug (Perkin Elmer) and then dispersing them in low density polyethylene
powder. The mixture was then melted between two glass plates at ca 100°C, to
form nearly clear plate-shaped samples of about 6 cm^2 containing ca 15 weight
percent glass.

The far infrared spectra were measured on a Digilab FTS-15B Fourier
Transform infrared spectrometer equipped with a 6.25 µm mylar beam-splitter.
Each spectrum is the result of a signal averaging at least 400 scans at 4 cm^{-1}
resolution.

Spectral Results

Far Infrared Spectra

The far infrared spectra of both the SAGs and MAGs were studied to determine
the extent to which the cation-anionic site interactions, evaluated by analyzing
the cation motion bands, depend on the nature and the concentration of the cations

and the presence of a dissimilar cation.

The far infrared spectrum of each glass was measured both before and after annealing, but no significant differences were caused in the cation-motion spectra by the annealing treatment; so no distinction will be drawn between the spectra of the annealed and unannealed samples.

The far infrared spectra of the Na, K, Rb and Cs pentasilicate SAGs, shown in Figure 1, exhibit a broad band whose position and bandwidth are strongly cation-dependent. The band for the Na-glass is centered at 195 ± 15 cm^{-1}, while the bands for K, Rb and Cs are at 141 ± 5, 94 ± 4 and 69 ± 4 cm^{-1}. To illustrate the general dependence of the vibrational frequency on the cation the frequencies are plotted in Figure 2 versus $M_c^{-1/2}$, where M_c is the mass of the cation. Clearly, ν varies nearly linearly with $M_c^{-1/2}$, although $M_c^{-1/2}$ is not necessarily the appropriate form of the vibrational reduced mass. The bandwidth also changes systematically with cation, decreasing in the order Na > K > Rb > Cs. The spectrum of phase-separated $Li_2O\cdot5SiO_2$ is not shown in Figure 1, since it gave a very broad featureless absorption between 300-500 cm^{-1}.

The far infrared spectra of the Cs-Na MAGs are given in Figure 3. The cation-motion bands due to both Na and Cs are observed. As x increases from 0 to 1 their relative intensity changes. Thus, the broad featureless Na band gradually decreases in intensity, while the Cs-motion band grows in intensity and shows a direct dependence on Cs concentration. Each cation-motion band remains essentially unshifted in frequency within experimental error as x is varied. This is seen more clearly for Cs when the effect of the part of the background due to the Na band is removed.

Raman Spectra

The Raman spectra of SAG and MAG pentasilicate fibers and chips that have the same composition are essentially identical, so only the spectra of the chips

(SAGs and MAGs) and of the fully annealed cubes (MAGs) are reported.

Single Alkali Pentasilicate Spectra

The Raman spectra of alkali pentasilicate SAGs-chips in the 300-1300-cm^{-1} region are shown in Figure 4. The spectrum of fused silica, SiO_2, is included for comparison. It is clear that the spectra of these Cs, Rb, K and Na glasses are very similar, which indicates that there are not major differences in the network structure of these glasses. These four spectra in particular are similar to the spectra of $Na_2O \cdot 4SiO_2$ and $Na_2O \cdot 5.67\ SiO_2$ reported by White et al (24) and $Na_2O \cdot 4SiO_2$ reported by Mysen et al recently (25). They also are analogous to those of $K_2O \cdot 4SiO_2$ and $K_2O \cdot 3SiO_2$ reported by Konijnendijk and Stevels (26) and Iwamoto et al (27), respectively. The Raman spectrum of $Li_2O \cdot 5SiO_2$ glass has strong features resembling that of SiO_2, especially in the low frequency region. This glass is phase-separated and so there are SiO_2-rich regions, as seen by comparison with the vitreous SiO_2-spectrum, which compares well with those reported (28). Knowledge of the polarization characteristics of the Raman bands is important in assigning them, so the polarized spectra of these glasses also have been measured.

The bands appearing in the spectra of Figure 4 can be grouped conveniently into three frequency regions; low (300-700 cm^{-1}), middle (700-1000 cm^{-1}) and high (1000-1300 cm^{-1}). In the low frequency region the band at ca 600 cm^{-1} is polarized and appears at the same frequency (within experimental error) for all of the alkali pentasilicate glasses, while its intensity increases systematically from Na to Cs. A notable shift occurs for the next band in this region, the band ca 500 cm^{-1}, which also is polarized. As shown in Figure 5, this band shifts linearly with ionic radius (r), but it does not with either cation mass (M_c) or ionic potential (q/r). The significance of this distinction becomes apparent when the spectra of the mixed alkali glasses are presented, as in

Figure 5, for the band in this region since linear shifts with x would occur for the mixed alkali series whatever property is averaged. The peak of SiO_2 at 437 cm^{-1} is present in the spectra of Li and Na glasses of ca 440 cm^{-1}, but is absent in the spectra of K, Rb and Cs glasses.

In the high frequency region the spectra of Na, K, Rb and Cs glasses are very similar. The band at ca 1100 cm^{-1} is the most intense band of the spectrum and is polarized. Its frequency and intensity do not change much with cation. Another feature appearing together with the (1100)-cm^{-1} band is a shoulder at about 1150 cm^{-1}. To obtain more information about the peak frequency and relative intensity of the band giving rise to this shoulder, the 1000-1200 cm^{-1} region should be deconvoluted. White et al (24b) deconvoluted the corresponding region of $Na_2O \cdot 3SiO_2$ into two bands, while Mysen et al (25) found still another weak band at ca 1050 cm^{-1} for $Na_2O \cdot ySiO_2$, y = 2,3,4. Therefore, to set the criteria for the number of bands to be found by deconvolution of the (1100)-cm^{-1} band, we decided to establish whether its low frequency side matches the shape of a single Raman band, or whether there is indeed a third band at ca 1050 cm^{-1}, as concluded by Mysen et al.

The most commonly used functions to describe Raman band shapes are the Gaussian (29)

$$F(\nu) = F_{max} \exp \frac{-\ln 2(\nu - \nu_o)^2}{\Gamma^2} \tag{1}$$

and Lorentzian (29)

$$F(\nu) = F_{max} \frac{\Gamma^2}{\Gamma^2 + (\nu - \nu_o)^2} \tag{2}$$

where ν_o is the band frequency, F_{max} is the peak height at $\nu = \nu_o$ and 2Γ is the full band width at half maximum (FWHM). If there is a band at ca 1050 cm^{-1} then this band should be resolved easier in the spectrum of $Na_2O \cdot 5SiO_2$ glass, since this spectrum shows the broadest (1100)-cm^{-1} band. At this point we make the

tentative assumption that the part of the low frequency side from the peak maximum to about half maximum represents a single Raman band. Then we use the FWHM, $2\Gamma = 78$ cm^{-1}, $\nu_o = 1093$ cm^{-1}, and $F_{max} = 178$ (arbitrary units) of the Na(1100)-cm^{-1} band to generate the low frequency side of the (1100)-cm^{-1} band, by employing Eqns (1) and (2). The results are given in Figure 6. The experimental band fits the Lorentzian function very well from about 1040 cm^{-1} to the peak frequency and deviates in the wings, while the fit to the Gaussian function is not as good as that to the Lorentzian function. The deviation in the wings is opposite to that of the Lorentzian function. These results indicate that there is no 1050 cm^{-1}, since the presence of such a band would make the wings of the (1100)-cm^{-1} band show a positive deviation relative to both Lorentzian and Gaussian function.

The deconvolution of the (1100)-cm^{-1} band is then done graphically and the polarized (1150)-cm^{-1} band is found at 1163, 1156, 1155 and 1152 cm^{-1} for the Na, K, Rb and Cs glasses respectively. The FWHM of the deconvoluted (1100)-cm^{-1} band is plotted in Figure 7 versus cation radius, (r). A systematic sharpening of this band is affected by increasing cation size. A similar trend was observed for other silicate glasses (24). In addition, the intensity of the deconvoluted (1150)-cm^{-1} shoulder relative to the (1100)-cm^{-1} band increases as r increases.

In the middle frequency region the spectra of Li and Na glasses exhibit a polarized peak at 950 cm^{-1}, while the rest of the pentasilicates show a weak band at ca 980 cm^{-1}. The depolarized band at ca 800 cm^{-1} is common to all spectra, and its frequency at maximum intensity also is given in Figure 5 versus r, where it shows a nearly linear decrease with r. Another feature of this band is that it becomes broader as the larger cation enters the network, while its height decreases in the same order.

The high frequency part of the SiO_2 spectrum is characterized by two bands at 1195 and 1056 cm^{-1}. The Li glass shows a band at 1078 cm^{-1}, whose relative intensity is small compared to that of the (1100)-cm^{-1} band of the other pentasilicates. Obviously this is so because the Li glass is phase separated and thus the 1078-cm^{-1} band resembles more the 1056-cm^{-1} band of SiO_2 than the (1100)-cm^{-1} band of Na, K, Rb and Cs glasses.

Mixed Alkali Pentasilicate Spectra-Chips

The Raman spectra of pentasilicate MAGs-unannealed chips are shown in Figure 8. Comparison of these spectra with those of SAGs (Figure 4) shows a general similarity with some exceptions in the (800)-cm^{-1} band region. The (600)-cm^{-1} band does not shift in frequency, but its relative intensity increases systematically with x. The (500)-cm^{-1} band shifts linearly to lower frequencies as x is varied from zero to one, as shown in Figure 9. This x dependence of $v(500)$ cm^{-1} is really a size rather than a mass or field strength dependence, as shown characteristically by Figure 5 for the corresponding band of pentasilicate single alkali glasses.

The (1100)-cm^{-1} band does not change significantly in frequency with x, but it becomes sharper upon increasing x, as shown in Figure 7 where its bandwidth, FWHM, is plotted versus r_{eff}. Here r_{eff} equals $xr_{Cs} + (1-x)r_{Na}$, where r_{Cs} and r_{Na} are the radii of Cs^+ and Na^+ respectively. Also the (1150)-cm^{-1} shoulder increases in intensity as x varies from 0 to 1.

The middle frequency region depends strongly on x. The 950-cm^{-1} band is observed only in the case where x = 0. In addition, the shape and intensity of the (800)-cm^{-1} band changes dramatically as x is varied, that is, it becomes very broad and rather strong for x = 0.4, 0.5, and 0.6. There is a maximum in its FWHM at ca x = 0.5. The difference between the FWHM value at x = 0.5 and the average value of the end member glasses (x = 0 and x = 1) is about 115%.

The FWHM of the (800)-cm^{-1} band of the single alkali pentasilicate glasses changes linearly with x_{eff}, stated as $x_{eff} = (r_M-r_{Na})/(r_{Cs}-r_{Na})$. Thus the main difference between the spectra of SAGs and MAGs (chips) is the significant broadening of the (800)-cm^{-1} band, in MAGs, as x approaches 0.5.

Mixed Alkali Pentasilicate Spectra - Cubes.

The Raman spectra of the cube-shaped (carefully annealed) MAGs are shown in Figure 10. Comparison of these spectra with those of SAGs reveals close similarities in both band shapes and relative intensities. The most important difference between these spectra (Figure 10) and those of the chip - MAGs (Figure 8) occurs in the (800)-cm^{-1} region.

The variation with r of the bandwidth of the (1100)-cm^{-1} band is given in Figure 7. The same trend is observed in both cubes and chips, but the bandwidth is a little smaller in cubes than in chips. The deconvolution of the (1150)-cm^{-1} shoulder gave peaks of 1163, 1163, 1162, 1163, 1163, 1155 and 1152 cm^{-1} for x = 0, 0.2, 0.4, 0.5, 0.6, 0.8 and 1.0 respectively.

The frequency of the (500)-cm^{-1} band is plotted vs x in Figure 9, which shows, by comparison, that frequency values are the same as those of chips. The variation of the FWHM of the (800)-cm^{-1} band of cube samples with x also has been evaluated. As in the case of the chips, a maximum also appears at x = 0.5 for the cube samples, but now the difference between the maximum value and the average value of the end members is only about 7%, while it was 115% for chips. Thus analogous variations of FWHM occur in both cube and chip series, but it is more pronounced in the chip series than in cubes.

The main difference between the two series (chip and cubes) was the rate of cooling of the melt and the subsequent annealing treatment. The chips were essentially quenched from the melt and left unannealed, while the melts forming

the cubes reached room temperature very slowly, and then the resulting glasses were annealed at about T_g. If quenching the chips without annealing is the main reason for the differences in the $(800)-cm^{-1}$ region, then annealing of the chips should make their structural characteristics approach those of the cubes of the same composition. The results of such annealing are given in the next section.

Annealing Effects on Chips MAGs.

Annealing was performed on chips for both SAGs and MAGs by heating the samples at about T_g for 15 h, and then cooling the samples to room temperature at a rate of ca 1°C min^{-1} over a period of ca 7 h.

The Raman spectra of pentasilicate SAGs did not show large changes after annealing. White et al. (24b,30) reported that although annealing the $Na_2O \cdot 5.67SiO_2$ glass for 10 h did not affect its Raman spectrum, annealing $Na_2O \cdot 4SiO_2$ caused its 520 cm^{-1} band to split into two bands at 530 and 495 cm^{-1} while the high frequency bands remained unchanged. This splitting of the 520 cm^{-1} band was interpreted as indicating the onset of phase separation caused by annealing. The pentasilicate SAGs, like $Na_2O \cdot 5.67SiO_2$, remain unchanged after heat treatment.

Annealing of the pentasilicate MAGs - chips caused changes in their Raman spectra. Representative spectra which illustrate this annealing effect are shown in Figure 11 for the MAG - chip of composition x = 0.5. The spectrum of the sample before annealing is denoted by a and the spectra measured after annealing for 15 h and 30 h, respectively, are denoted by b and c in Figure 11. The region around 510 cm^{-1}, whose band splitting is indicative of phase separation, remains unchanged upon annealing. One minor change observed is that the relative intensity of the 595-cm^{-1} band decreases upon annealing. This is similar to the reported decrease of the intensity of the 604-cm^{-1} band of SiO_2 upon annealing (31).

The (800)-cm^{-1} region of the Raman spectrum is the one most affected by annealing. While the high and low frequency regions of spectra a, b and c are almost identical, with the exception of the behavior of the 595 cm^{-1} band, a systematic decrease in the bandwidth of the 775 cm^{-1} band occurs upon annealing, so that spectrum c comes to resemble the spectrum of the cube sample of composition $x = 0.5$.

The general trends observed upon annealing for $x = 0.5$ were also observed for the rest of the MAG - chips. The change is less pronounced for $x = 0.2$, 0.0 and 1.0 and more pronounced for the intermediate compositions, $x = 0.5$, 0.4, 0.6 and 0.8. Upon annealing the Raman spectral behavior of the (800)-cm^{-1} band for the chips approaches that of the corresponding band of cubes. Its FWHM and the difference between it and that of the cubes always has its maximum at $x = 0.5$. To illustrate the effect of annealing further, the FWHM of the (800)-cm^{-1} band versus annealing time is plotted in Figure 12 for $x = 0.5$. Clearly, annealing this chip $(x = 0.5)$ for about 50 h is required to reduce the bandwidth of the (800)-cm^{-1} band to the value of the corresponding band for the cube of the same composition.

Discussion

Far Infrared Results

The far infrared spectrum of each pentasilicate single alkali glass exhibits one broad band whose frequency and bandwidth are strongly cation-dependent. Similar bands in the spectra of other glasses have been assigned to vibrations of cations in their sites (11,14,32). There is a range of such sites in glasses and each exerts forces similar to those at the corresponding crystal sites, so the cation motion band is the envelope of bands due to individual cation-site interactions. The decrease of the bandwidth in the order Na > K > Rb > Cs indicates that the smaller the cation the wider the range of interactions between

the individual sites and/or the broader the distribution of these sites. In other words, the cation-motion band is assigned to a large collection of coupled oscillators, which is equivalent to a single damped harmonic oscillator (11). The damping of the single oscillator comes from the coupling of the many individual oscillators. The strength of the cation-anionic site interactions is proportional to cation-motion associated force constant, $K = 4\pi^2 \mu c^2 \nu^2$, where μ is the reduced mass, c is the speed of light and $\nu(cm^{-1})$ is the cation-motion frequency. To calculate the reduced mass μ, we assume that the geometry of the oxygens around the cation can be taken as octahedral (11). The only infrared allowed stretching mode of a cation in an octahedral site is the T_{1u} mode, with reduced mass $\mu = \frac{M_c M_o}{M_c + 2M_o}$. Here M_c and M_o are the masses of the cation and oxygen respectively. Using this form of reduced mass we calculate the force constants to be 0.15×10^5, 0.103×10^5, 0.061×10^5 and 0.036×10^5 dyn cm^{-1} for the Na, K, Rb and Cs cation-motion bands, respectively. Thus, the cation-network interactions decrease in the order Na > K > Rb > Cs.

In the far infrared spectra of pentasilicate MAGs two different bands are shown, with intensity varying as the concentration of the appropriate cation. The frequency of the bands remains essentially unchanged with composition. This indicates that each cation is in a well defined site or range of sites, which is spectroscopically the same in single and mixed alkali glasses.

Terai and coworkers (15,16) have measured the self-diffusion coefficients of Na$^+$ and Cs$^+$ ions, as well as the electrical conductivities of glasses in the Na-Cs pentasilicate MAG system. They attributed the maximum in the activation energy for electrical conductivity at $x \cong 0.5$ to an increase of the alkali-oxygen bond strength that arises from the congregation of dissimilar alkali ions. Weyl and Marboe (33) and Mazruin (34) also postulated an increased oxygen-alkali bond strength as the primary cause of the mixed alkali effect. This increase of the oxygen-alkali bond strength is said to be due to differences

in mass (33) or differences in field strength (34) between the alkali ions. If
the change of electrical conductivity by orders of magnitude as x approaches 0.5
is really due to an increase of the alkali-oxygen bond strength then this effect
would manifest itself by a significant shift of the cation-motion band to
higher frequencies as x approaches 0.5. However, these experimental results
on pentasilicate MAGs, as well as those on metaphosphate MAGs (12), show the
opposite; namely, that the cation-motion bands in the far infrared spectra do
not shift with x. Thus the net force felt by a particular cation is largely
unaffected by the presence of the second cation. As noted in the Introduction,
experimental results of Berstein, et al (23) indicate that the M...O distance
is less in MAGs than in SAGs. If this decrease in distance reflects also
an increase in M...O bond strength, then it also is not in agreement with our
far infrared results. Finally, the cation-network interactions are found to
be largely unaffected by annealing.

Raman Results

Single Alkali Pentasilicate Glasses

Understanding the features of the Raman spectra of pentasilicate glasses,
and their dependence on composition, requires assigning the bands to specific
modes. This will be done in light of our results and assignments reported
for other silicate glasses.

Bell and coworkers (35) calculated the vibrational spectrum of SiO_2 with
a random network model. The main bands in the computed spectrum were found
at 400-500, 700-800 and 1000-1100 cm^{-1} in good agreement with the experimental
results. The high frequency band (ca 1100 cm^{-1}) was assigned to a bond-stretching
vibration in which the oxygen atoms move in an opposite direction to their silicon
neighbors and roughly parallel to the Si-Si lines. The band at about 800 cm^{-1}
was assigned to bond-bending type motion in which the oxygen atoms move at right

angles to the Si-Si lines and in the Si-O-Si plane. The 400-500 cm^{-1} peak was associated with a bond rocking motion of oxygen perpendicular to the Si-O-Si plane. The 605-cm^{-1} band of the Raman spectrum of SiO_2 is not predicted by the model.

Galeener and Lucovsky (36) suggested that the bands of the Raman spectrum of v-SiO_2 at 1195 and 1056 cm^{-1} result from LO and TO splitting, while Mysen et al (25,37) argued that such a splitting would require long range order that is not present in SiO_2 glass. Instead, they suggested that the two bands are due to two distinct three-dimensional structural units, and specifically that v-SiO_2 is characterized by a bimodal distribution of Si-O-Si angles in the three simensionally interconnected rings.

The origin of the 605-cm^{-1} band, of v-SiO_2, has been the subject of considerable discussion. It usually has been associated with "defect" structures in v-SiO_2, most commonly to broken Si-O bridging bonds in a continuous three-dimensional network (31,38,39). Lucovsky (38) assigned it to motion of Si-O$^-$ bonds relative to other Si-O bonds, and Stolen and Walrafen (31) reported that it is very sensitive to water content of v-SiO_2. Very recently Galeener argued that 2- and 3-fold rings should be present in v-SiO_2 and assigned this "defect" 605 cm^{-1} line to 3-fold planar rings (40).

There have been a number of approaches to interpreting the vibrational spectra of silicate glasses. Hass' (28c) assignments for the Raman spectra of sodium silicate glasses are similar to those of Bell and coworkers on SiO_2. The band at 1100 cm^{-1} was attributed to bond stretching of Si-O$^-$ and Si-O-Si bridging groups, and the band at 800 cm^{-1} was assigned to bending motions described by Bell. The 435- and 495-cm^{-1} bands were taken as characteristic bands of SiO_4 tetrahedra without non-bridging oxygens (NBOs). White and coworkers (24,41) compared the Raman spectra of silicate glasses to those of the corresponding crystalline compounds. By introducing defects and disordered units into the crystal structure conceptually and then doing a vibrational computation on the result, they predicted Raman spectra for the glasses (24b,42). It was suggested that the

950-cm^{-1} band in the disilicate and trisilicate glasses occurs because of the "fluctuations" in the number of NBOs per silicon tetrahedron and the band was assigned to tetrahedra with two NBOs (metasilicate structure) (24,41). This is consistent with the fact that the 950-cm^{-1} band is the strongest bond of the Raman spectrum of crystalline metasilicates.

Konijnedijk and Stevels based their assignments for silicate glasses on the vibrations of three units: SiO_2, $Si_2O_5^{2-}$ and SiO_3^{2-} with zero, one and two NBOs respectively (26,43). Virgo et al (44) assigned the 800-cm^{-1} band to a bending mode similar to that suggested by Bell and coworkers, while the 470-500 cm^{-1} region was attributed to bond-rocking in a three dimensional SiO_2 network.

The bands in the high frequency region of the Raman spectra of penta-silicate glasses clearly can be assigned to silicon-oxygen stretches. Specifically we assign the shoulder at ca 1150 cm^{-1} to symmetric Si-O$^-$ stretches (NBO) and the band at ca 1100 cm^{-1} to symmetric Si-O stretches involving bridging oxygens. The Si-O$^-$ band is expected to be stronger than the Si-O band because of $p\pi$-$d\pi$ back donation (45), and in fact this was supported by ESCA studies on alkali silicate glasses (46). The assignments of these bands as symmetric stretches is justified by the experimental evidence that both of them are strongly polarized.

The FWHM of the (1100)-cm^{-1} band, shown in Figure 7, decreases nearly linearly from Na to Cs. A similar trend was observed in other alkali-silicate glasses (24) and was interpreted as possibly meaning that the "order" of the Si-O network (for example, distribution of the Si-O bond lengths or relative orientations of the SiO_4 tetrahedra) increases with decreasing field strength of the cation. This is consistent with our assessment, discussed later, that the cation plays an important role in determining the structures assumed by the glass as it is formed in the transformation region. The effect of the cation on the Si-O$^-$ bond is expected to be greater than on the Si-O bond.

The higher the cation field strength is the more difficult it should be to polarize the Si-O$^-$ bond in the presence of the cation. The Raman scattering intensity is proportional to the square of the polarizability change and so the field strength differences should be reflected in Raman intensity differences for the Si-O$^-$ stretching.   In fact the relative intensity of the (1150)-cm^{-1} band does increase with decreasing cation-field strength.

In the middle frequency region, we attribute the (800)-cm^{-1} band to bending motions of Si-O-Si in accord with the assignment of Bell et al (35). The Si-O-Si angle should increase on average as the cation is varied from Na to Cs, and this should cause the bending mode frequency to decrease in that order (Figure 5). This also would be expected from the relation (38): $\nu^2(B) = (2k_r/M_o)(\cos^2\alpha + 2\gamma\sin^2\alpha)$ where $\nu(B)$ is the bending frequency, M_o is the mass of oxygen, 2α is the Si-O-Si bond angle, and γ is the ratio of the bond-bending to bond-stretching (Si-O) force constants, $\gamma = k_\theta/k_r$.

The (800)-cm^{-1} band is asymmetric and skewed to the high frequency side, as shown in the Raman spectra of v-SiO$_2$ and single alkali pentasilicate glasses (Figure 4). Its asymmetry in the case of v-SiO$_2$ was attributed by Mysen and coworkers (37) to the existence of more than one type of 3-dimensional unit in the melt. This explanation is supported by recent refinements of the random network model performed by Soules (47,48). Thus, it was shown that the calculated Si-O-Si angle distribution is asymmetric in v-SiO$_2$, and addition of Na causes a second peak to appear, near 110°, while the peak for SiO$_2$ occurs at about Si-O-Si = 150°. With increasing temperature the low angle peak in the Si-O-Si angle distribution disappears. The asymmetry of the Si-O-Si bond angle distribution at the low angle side would cause an asymmetry in the high frequency side of the bending mode of this bond (at ca 800 cm^{-1}), as exhibited by the corresponding mode of v-SiO$_2$ and pentasilicate SAGs.

Mixed Alkali Pentasilicates

Since the spectral assignments discussed in the previous section for SAGs are the same for MAGs, we will consider here only certain of the features observed in the spectra of MAGs.

One important observation in the Raman spectra of MAGs is that in each spectral region there is only one band of each kind. For example, there is only one (500)-cm^{-1} band whose frequency changes smoothly with x (Figure 9). If there were regions rich in a particular cation then they would cause (and could appear as) two bands of the same kind, one for each domain. That this is not the case, suggests strongly that the two different cations are randomly and uniformly distributed in the mixed alkali glass, and consequently, that the network feels an averaged cation-effect. This evidence for a statistical distribution of alkali ions is of particular importance, because some of the theories developed to explain the mixed alkali effect in electrical conductivity (3,4) have been based on special types of distributions of the alkali ions between alkali-rich and alkali-poor regions of the glass. Taken to its extreme this leads to phase separation, but to whatever extent it is taken the ion transport is limited by concentration gradients. However, the Raman results on pentasilicate MAGs show that such special types of distributions of alkali ions cannot provide the explanation of the MAE in electrical conductivity.

As mentioned in the Introduction it has been reported (23) that the Si-O bond is stronger in MAGs than in SAGs. As shown in Figures 8 and 10 the (1100)-cm^{-1} band is a few cm^{-1} higher in frequency in MAGs than SAGs, but the difference is not large enough to be conclusive about the strength of the Si-O bond. Moreover this small shift of the stretching frequency of Si-O could be due to a number of other small effects, such as changes in the Si-O-Si angle, rather than to a

significant change in the force constant of the Si-0 bond.

The (800)-cm^{-1} band of mixed alkali glasses (unannealed chips) is broadened significantly as x approaches 0.5 (Figure 8). As discussed above, this is a consequence of broadening of the distribution of Si-0-Si angles. The band becomes more skewed toward high frequency as x varies from 0 to 0.5. This suggests that the distribution of Si-0-Si angles in mixed alkali pentasilicate glasses broadens more towards smaller than towards greater Si-0-Si angles, relative to that of single alkali glasses. This also is consistent with calculations of the energies of various model systems, such as the $(OH)_3Si-0-Si(OH)_3$ molecule, as a function of the bridging angle, Si-0-Si = θ. The result (49) is that the energy of the system increases as θ deviates from the equilibrium angle, of course, and that it increases faster as θ shifts to smaller angles. Deviations from the equilibrium θ result in increased strain energy.

The mixed alkali glass with composition x = 0.5, exhibits the broadest Si-0-Si angle distribution as shown by the Raman spectra and therefore should have the maximum inherent strain. This strain is the result of network deformations (for example, deviations), since the network is forced to somehow rearrange its structure in order to accommodate the size mismatch of dissimilar cations in neighboring anion sites. The differences in strain in MAGs, postulated in (21) to explain the x-dependence of the activation energy for the HTP, of the mechanical spectrum, is in accord with these experimental results.

Another property which may be affected by the distribution of Si-0-Si angles is the isothermal compressibility. From volume considerations it is expected that the unit with the larger Si-0-Si angle is more compressible than that with the smaller Si-0-Si angle (37). Thus the glass with the biggest number of units with small Si-0-Si angles is expected to show the smallest compressibility. This is, in fact, one of the results we obtained from the Brillouin study on the Na-Cs MAGs. A similar explanation can be given for the x-dependence of the isothermal compressibility of pentasilicate MAGs, if one considers the

ability of the network to undergo structural rearrangements as the main source of isothermal compressibility. The network which has been already forced to do some of these rearrangements (bigger Si-O-Si angle distribution to accommodate different size cations), has lost a part of its ability (degrees of freedom) for further rearrangements, and so this network (x = 0.5) shows minimum in isothermal compressibility.

It is shown, Figs. 8,10, that the distributions of Si-O-Si angles (and consequently the strain introduced) is greater in chips (annealed) than in cubes (annealed). Upon annealing, the angle distribution in chips becomes narrower and approaches that of cubes. This is consistent with the fact that the low angle peak in the Si-O-Si bond angle distribution decreases in intensity with increasing temperature, and finally disappears at high temperatures (47). The result that there is some additional angle distribution (strain) left in the cube specimens (annealed), simply indicates that this residual strain cannot be completely relieved by annealing and reflects the effect of size mismatch of the dissimilar cations. This strain induced by cation size differences in MAGs manifests itself in the variation of the isothermal compressibility with x and in the HTP behavior of the mechanical spectra of MAGs.

In conclusion, we have shown the following in this study. First, the vibrationally significant cation-network interactions for a particular cation are not affected by the introduction of a dissimilar cation or by annealing. Thus, establishing the optimum cation-site geometry may be the first requirement satisfied as glass formation occurs, i.e. it may be the one most favored energetically. Second, the cations are statistically distributed throughout the network in MAGs and thus the network is associated with an average environment which changes smoothly with x in a series of MAGs. Third, the size difference of dissimilar cations in MAGs introduces a broadening of the Si-O-Si

angle distribution into the network, which is only partially relieved by annealing. And, fourth, the composition dependence of some properties of MAGs, such as isothermal compressibility and HPT activation energy, can be understood on the basis of additional Si-O-Si angle distribution-strain induced by the size difference of the alkali ions.

Acknowledgment

References

1. J.O. Isard, J. Non-Crystalline Solids, 1, 235 (1969).

2. D.E. Day, J. Non-Crystalline Solids 21, 343 (1976).

3. R.L. Myuller, Sov. Phys-Solid State 2, 1219, 1224 (1960).

4. R.J. Charles, J. Am. Ceram. Soc. 48, 432 (1965) and Glass. Technol.
    12, 24 (1971).

5. J.M. Stevels, The Electrical Properties of Glass, in
    "Handbuch der Physik", Band 20,Ed. S. Flügge, Springer-Verlag, Berlin,
    1957.

6. J.R. Hendrickson and P.J. Bray, Phys. Chem. Glasses, 13, 43, 107 (1972).

7. G.B. Rouse, J.M. Gordon and W.M. Risen, J.Non-Crystalline Solids 33, 83
    (1979).

8. V.N. Filipovish, Sov. J. Glass Phys. and Chem. 6, 245 (1980).

9. A.T. Tsatsas, J.W. Reed and W.M. Risen, J. Chem. Phys. 55, 3260 (1971).

10. A.T. Tsatsas, R.W. Stearns and W.M. Risen, J. Am. Chem. Soc. 94, 5247 (1972).

11. G.J.Exarhos, P.J. Miller and W.M. Risen, J. Chem. Phys. 60, 4145 (1974).

12. G.B. Rouse, P.J. Miller and W.M. Risen, J. Non-Crystalline Solids 28,
    193 (1978).

13. G.B. Rouse, E.I. Kamitsos and W.M. Risen, J. Non-Crystalline Solids 45,
    257 (1981) and 46, 441 (1981).

14. G.J. Exarhos and W.M. Risen, Solid State Commun. 11, 755 (1972)

15. R. Terai, J. Non-Crystalline Solids, 6, 121 (1969).

16. R. Hayami and R. Terai, Phys. Chem. Glasses, 13, 102 (1972).

17. R. Terai, M. Hori and H. Yamanaka, Amer. Ceram. Soc. Bull. 58, 1125 (1979).

18. W.E. Steinkap, J.E. Shelby and D.E. Day, J. Am. Ceram. Soc. 50, 271 (1967).

19. J.W. Fleming and D.E. Day, J. Am. Ceram. Soc. 55, 186 (1972).

20. a) J.E. Shelby and D.E. Day, J. Am. Ceram. Soc. 52, 169 (1969); 53, 182
    (1970) and b) H.M. Van Ass and J.M. Stevels, J. Non-Crystalline Solids, 15,
    215 (1974); 16, 46 (1974).

21. C.H. Tzinis, Ph.D. Thesis, Brown University 1981.

22. C.Windisch and W.M. Risen, J. Non-Crystalline Solids, 44, 345 (1981).

23. V.A. Berstein et al, J. Non-Crystalline Solids, 38/39, 141 (1980).

24. a) S.A. Brawer and W.B. White, J. Chem. Phys. 63, 2421 (1975) and b) T. Furukawa, K. Fox and W.B. White, J. Chem. Phys. 75, 3226 (1981).

25. B. Mysen et al, American Mineralogist 65, 690 (1980).

26. W.L. Konijnendijk and J.M. Stevels, J. Non-Crystalline Solids 21, 447 (1976).

27. N. Iwamoto et al, J. Non-Crystalline Solids, 18, 303 (1975).

28. a) F. Flubacher et al, J. Phys. Chem. Solids, 12, 53 (1959); b) M.C. Tobin and T. Baak, J. Opt. Soc. Am. 58, 1459 (1968) and c) M. Hass, J. Phys. Chem. Solids 31, 415 (1970).

29. M.C. Tobin, "Laser Raman Spectroscopy", Wiley-Interscience, New York 1971

30. W.B. White, J. Non-Crystalline Solids 49, 321 (1982).

31. R.H. Stolen and G.E. Walrafen, J.Chem. Phys. 64, 2623 (1976).

32. G.J. Exarhos, Ph.D. Thesis, Brown University, 1974.

33. W.A. Weyl and E.C. Marboe, in "Constitution of Glasses", Vol. II, Part 1. Interscience Publishers, John Wiley and Sons, Inc. New York 1964.

34. O.V. Mazurin, in "Structure of Glass" Vol. IV, Consultants Bureau, New York 1966.

35. R. Bell et al, J. Phys. C: Solid State Phys. 3, 2111 (1970); 4, 1214 (1971); R. Bell and Dean, Disc. Faraday Soc. 50, 55 (1970) and R. Bell and Dean, in "Amorphous Materials" Eds. R.W. Douglas and B. Ellis, Wiley Inter-Science, New York, 1972.

36. F.L. Galeener and G. Lucovsky, Phys. Rev. Lett. 37, 1474 (1976).

37. F. Seifert, B.O. Mysen and D. Virgo, American Mineralogist, 67, 696 (1982).

38. G. Lucovsky, Phil. Mag. 39, 513, 531 (1976).

39. J.B. Bates et al, J. Chem. Phys. 61, 4163 (1974).

40. F.L. Galeener, J. Non-Crystalline Solids, 49, 53 (1982).

41. S.A. Brawer and W.B. White, J. Non-Crystalline Solids, 23, 261 (1977).

42. S.A. Brawer, Phys. Rev. B11, 3173 (1975).

43. W.L. Konijnendijk, Philips Res. Repts. Suppl. No. 1 (1975).

44. D. Virgo et al, Carnegie Inst. of Washington Year Book 78 (1979) and

    D. Virgo et al, Science 208, 1371 (1980).

45. K.A.R. Mitchell, Chem. Rev. 69, 157 (1969).

46. R. Brückner et al, Glastechn. Ber. 51, 1 (1978); and J. Non-Crystalline

    Solids 42, 49 (1980).

47. T.F. Soules, J. Chem. Phys. 71, 4570 (1979).

48. T.F. Soules, J. Non-Crystalline Solids, 49, 29 (1982).

49. A.R. Revesz and G.V. Gibbs, in "The Physics of MOS insulators", eds. G.

    Lucovsky, S.T. Pantelides and F.L. Galeener, Pergamon Press, New York 1980.

Figure Captions

Figure 1. The far-infrared spectra of single alkali pentasilicate glasses: $M_2O \cdot 5SiO_2$; where M = Na, K, Rb, Cs, as marked on the figure.

Figure 2. A plot of the cation-motion frequencies of the alkali pentasilicate glasses, $M_2O \cdot 5SiO_2$, versus $M_c^{-1/2}$, where M_c is the mass of the cation.

Figure 3. The far infrared spectra of mixed alkali pentasilicate glasses: $xCs_2O(1-x)Na_2O \cdot 5SiO_2$.

Figure 4. Raman spectra of single alkali pentasilicate glasses-chips.

Figure 5. Variation of the frequency of the (500)-cm^{-1} and (800)-cm^{-1} bands versus ionic radius (r), for SAGs: $M_2O \cdot 5SiO_2$.

Figure 6. Deconvolution of the high frequency Raman band of $Na_2O \cdot 5SiO_2$.

Figure 7. Bandwidth, FWHM, of the (1100)-cm^{-1} band versus r for $M_2O \cdot 5SiO_2$-chips, and versus r_{eff} for $xCs_2O(1-x)Na_2O \cdot 5SiO_2$-chips and cubes.

Figure 8. Raman spectra of mixed alkali pentasilicate glasses-unannealed chips.

Figure 9. Frequency of the (500)-cm^{-1} band versus x, for $xCs_2O(1-x)Na_2O \cdot 5SiO_2$ MAGs-chips and cubes.

Figure 10. Raman spectra of mixed alkali pentasilicate glasses-cubes.

Figure 11. Effect of annealing on the Raman spectrum of $0.5Cs_2O\ 0.5Na_2O \cdot 5SiO_2$-chip. Spectrum (a) is measured before annealing, spectrum (b) after

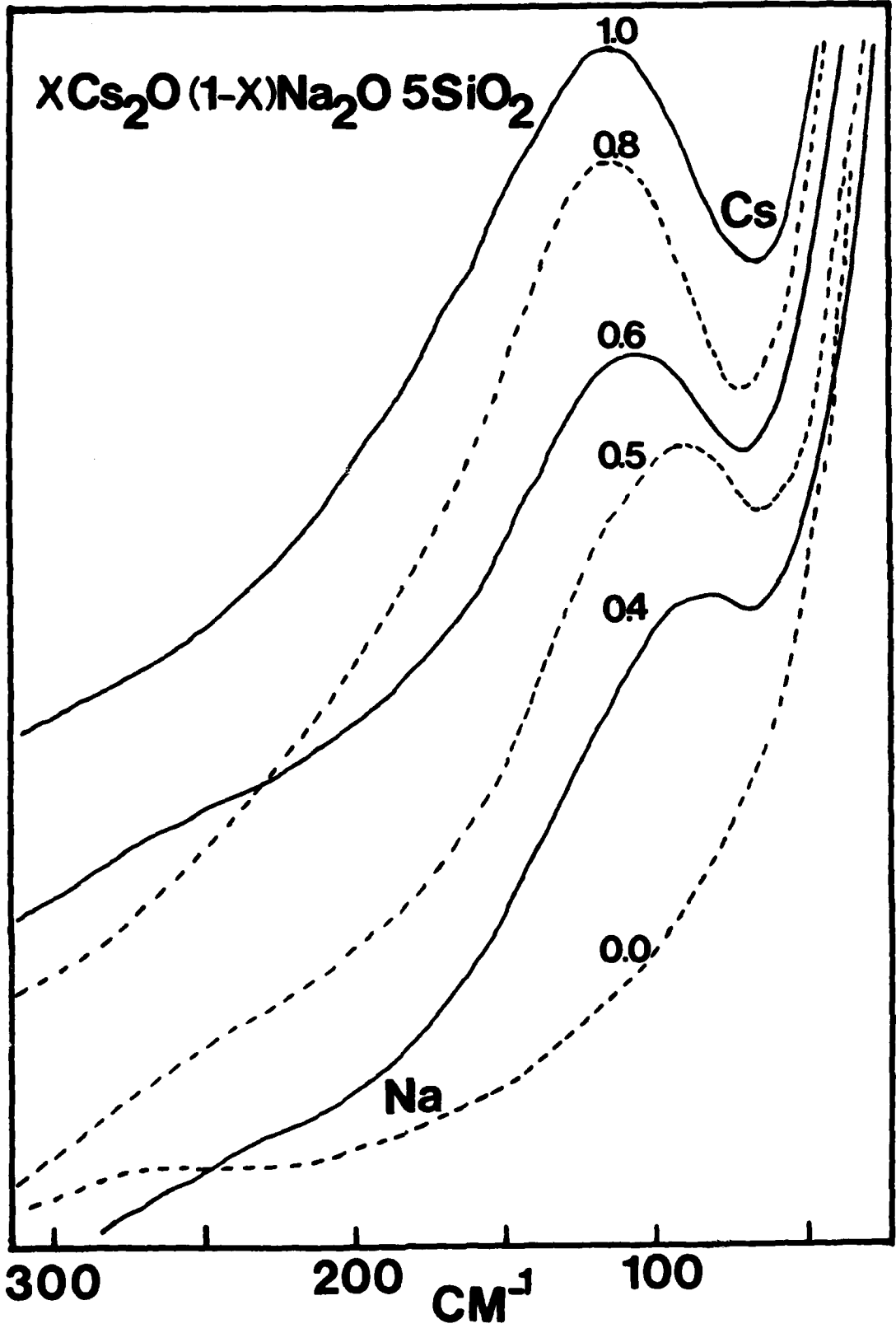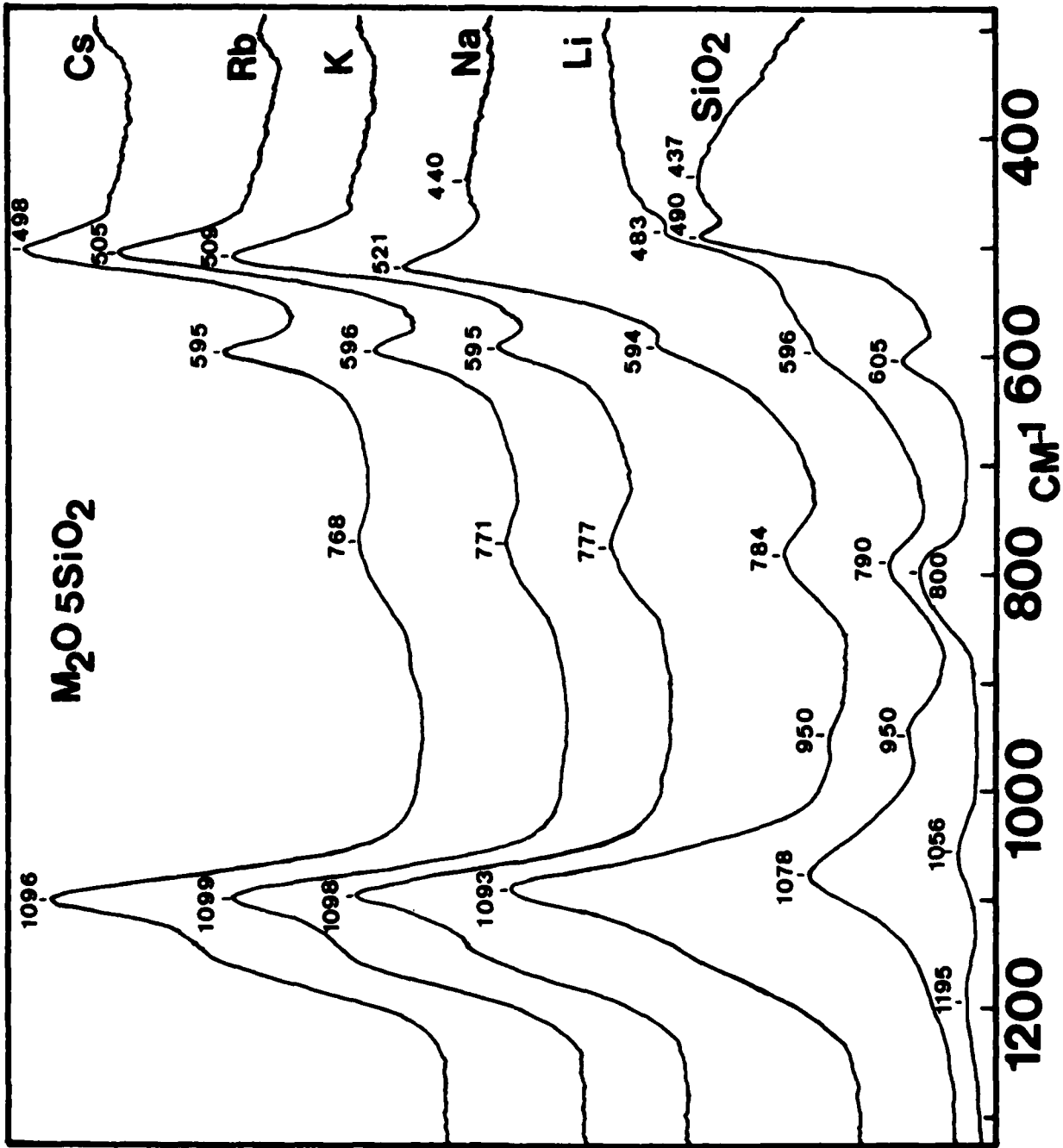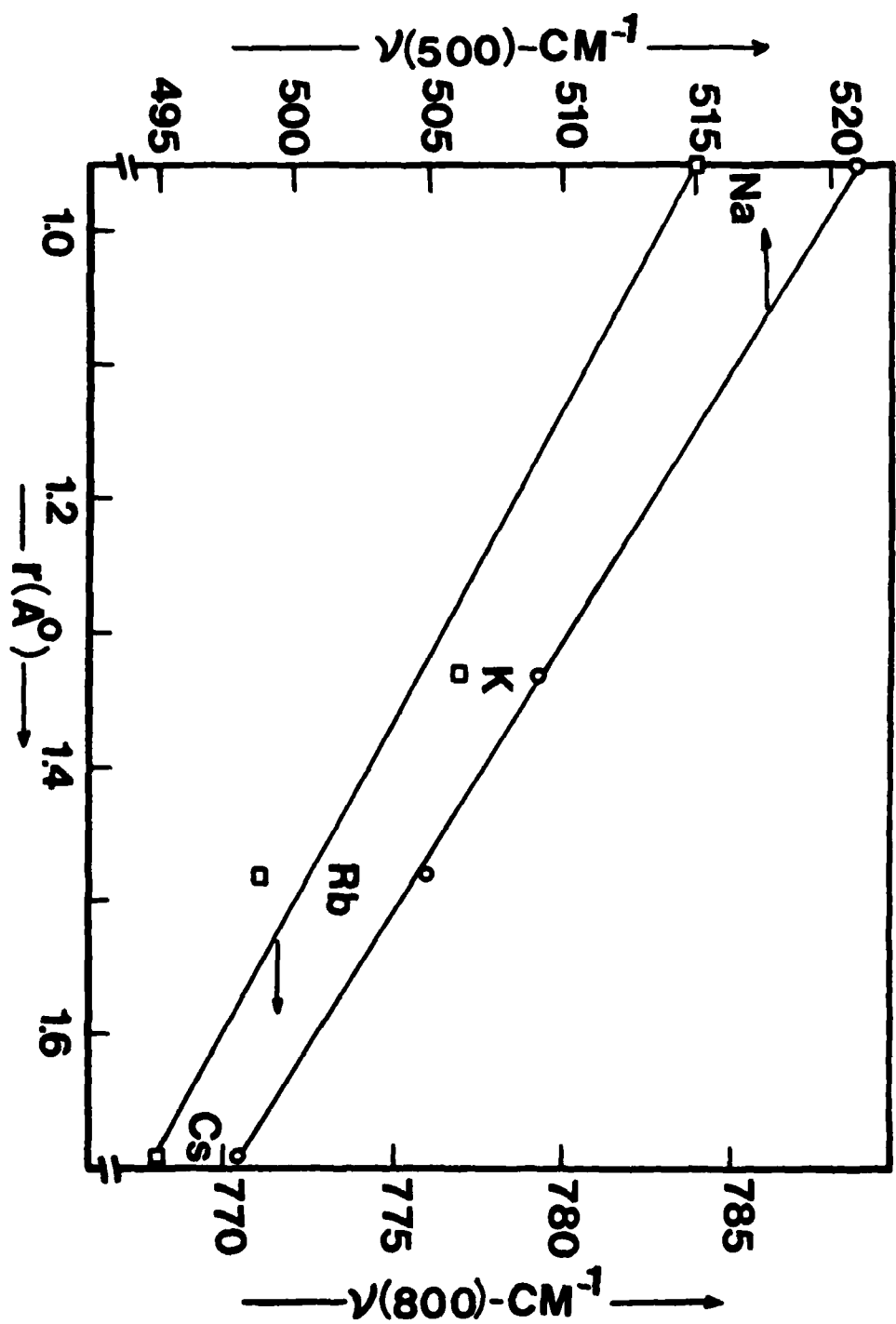annealing for 15 h, and spectrum (c) after annealing for 30 h.

Figure 12.   FWHM of the (800)-cm^{-1} band versus annealing time for $0.5Cs_2C$ $0.5Na_2O \cdot 5SiO_2$- chip

M$_2$O 5SiO$_2$

XCs$_2$O (1-X)Na$_2$O 5SiO$_2$

Cs
Rb
K
Na
Li
SiO$_2$

M$_2$O 5SiO$_2$

1498
505
509
440
483
490 437
SiO$_2$

595
596
595
594
596
605

768
771
777
784
790
800

950
950
1078
1056

1096
1099
1098
1093
1195

400   600   800   1000   1200

CM^{-1}

xCs_2O $(1-x)Na_2O$ $5SiO_2$ chips

xCs_2O $(1-x)Na_2O$ $5SiO_2$
cubes

0.5Cs$_2$O 0.5Na$_2$O 5SiO$_2$
chip

FWHM(800)-CM^{-1}

Annealing time (h)

cube x=0.5

END

FILMED

8-83

DTIC